

**Adaptation Strategies on Flexible Pavement Design Practices Due to Climate Change in  
Canada**

Paula Sutherland Rolim Barbi  
Ph.D. Candidate  
University of Waterloo

Guangyuan Zhao  
Research Associate  
University of Waterloo

Syeddata Nahidi  
Research Associate  
University of Waterloo

Jessica Achebe  
Ph.D. Candidate  
University of Waterloo

Susan Tighe  
Provost and Vice-President, Academic  
McMaster University

Paper prepared for Innovations in Pavement Management, Engineering and Technologies  
session of the 2021 TAC Conference & Exhibition

## **Abstract**

It has been shown that Canada's climate is warming at more than double the global rate [1], therefore, Canadian road infrastructure could be at risk if adaptation strategies are neglected. Key climatic parameters that govern the design and performance of flexible pavement may alter in the future, leading to different climatic loads on road structures, which in turn may result in reduced performance and shortened service life. To that end, this research aims to propose a methodology for the incorporation of climatic projected changes in the design of flexible pavement in Canada. To reach this goal, first, climate change projections over Canada will be evaluated and limitations of existing climatic data used for pavement structural design will be assessed; second, the impacts of climate change on pavement performance will be further discussed, followed by the introduction of a methodology to incorporate climate change predictions in pavement structural design; lastly, an example will be performed to illustrate the incorporation of the climate change parameters in the design procedure of AASHTO 93. The climatic inputs to be evaluated are temperature, precipitation, permafrost thawing, and freeze-thaw cycles. This study aims not only to provide guidelines for flexible pavement design but also to raise public awareness by engaging government and stakeholders across the country.

## **Introduction**

The 2019 Climate Change Report – CCCR2019 developed by the Government of Canada shows that Canada's climate is warming at more than double the global rate [1]. It is anticipated that heat waves will occur more often and last longer and that the potential rutting will increase with higher extreme in-service pavement temperatures [2]. Extreme precipitation events in many regions are more severe and frequent, which will lead to flood damage. At the same time, road structures will freeze later but thaw sooner with correspondingly shorter freezing periods in the evolving environments.

Road infrastructure is essential to the Canadian economy, as most goods and services are transported primarily by trucks and cars. These roads are highly vulnerable as they were not designed to tackle the changing climate conditions adequately. The concerns related to the changing climate in pavement design and management include reduced performance, loss of serviceability, shortened service life, more frequent maintenance and rehabilitation, higher construction and operation costs, and adverse socio-economic impacts on communities [3], [4], [5]. A comprehensive understanding of the effects of climate change on road infrastructure is, therefore, vital for decision-making that takes climate risks into account and improves adaptive planning.

In Canada, flexible pavement design methods vary in different provinces. In recent years, the Mechanistic-Empirical Pavement Design Guide (MEPDG) is becoming more common, however, the most common design method in Canada is still the 1993 AASHTO Guide for Design of Pavement Structures [5]. In the AASHTO 93 method, the climatic factors are not always used as a direct design input, however, the consideration of the climatic factors could be incorporated when selecting design inputs related to pavement materials and performance criteria. To that end, this research aims to propose a methodology for the incorporation of climatic projected changes in the design of flexible pavement in Canada. This methodology can be used as a guide for pavement designers in Canada to consider climate change in their practices.

## Climate Projections in Canada

### Temperature

In 2019, a detailed report concerning the temperature changes in Canada was published by Environment and Climate Change Canada. This report presented several crucial facts which later could affect the life cycle of the infrastructures and specifically pavements and roads. Based on this report, by analyzing the temperature data between 1948 to 2019, it can be concluded that the annual average temperature increased by 1.7°C.

It was also reported that the average spring and autumn temperature increased by 1.7°C from 1948 to 2019. Moreover, throughout the very same timeframe, winters got warmer by 3.3°C. The least change in seasonal average temperature was for summer with 1.4°C increase. The most changes in regional temperature were recorded in northern provinces and territories such as Yukon, Northwest Territories, and Nunavut. These changes can significantly reduce the thickness of glaciers, increase the sea levels and significantly endanger species [1].

The Government of Canada also developed an online tool with the ability to demonstrate possible scenarios of climate change in Canada. This tool projects twenty-year average changes in three different timeframes: Near term: 2016 to 2035, Mid term: 2046 to 2065, Long term: 2081 to 2100. Figure 1 shows the long term projected temperature changes in Canada [1].

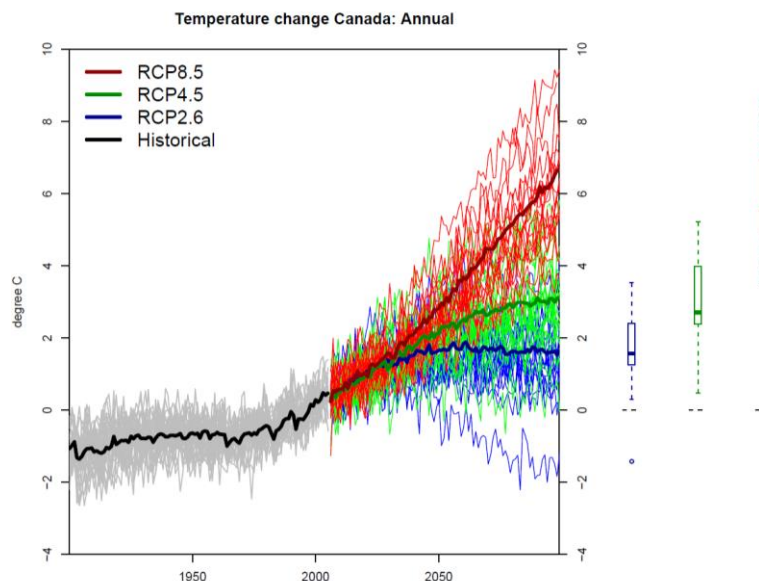


Figure 1: Projected Temperature Changes in Canada [1]

There are three emission scenarios presented in Figure 1, they are the Representative Concentration Pathway (RCP) 2.6, 4.5, and 8.5, in the sources of confidence of 25<sup>th</sup>, 50<sup>th</sup>, and 75<sup>th</sup> percentiles.

### Precipitation

Precipitation is the key component in human society and in development and sustainability of ecosystems. Changes in precipitation due to climate change could immensely impact the human society and ecosystems. Precipitation in Canada varies significantly due to wide-range

of temperature and diverse topography, resulting in annual precipitations that goes from more than 3000 mm to less than 200 mm in some areas [6].

Figure 2 presents a forecast of the mean precipitation in Canada under the same emission scenarios RCP2.6, 4.5, and 8.5. Based on historical data (left grey area of the graph), precipitation rate did not fluctuate significantly in the last century. However, under RCP8.5 scenario, a huge increment in precipitation rate is expected, and even in the most optimistic scenario the precipitation rate will increase by 2100.

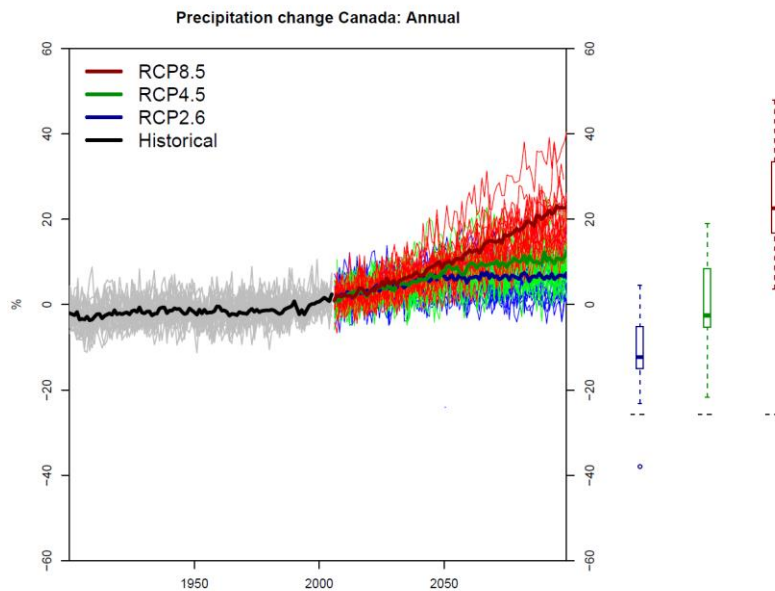


Figure 2: Projected Precipitation Changes in Canada [1]

Unlike trends in temperature changes in Canada, precipitation changes are not occurring in a systematic and detectable trend. Days with heavy rain and snow have increased by only 2 to 3 days in sites such as British Columbia, Ontario, and Quebec, and it is not consistent with the global findings [7]. However, since precipitation is highly dependent on temperature, it is believed that when the temperature gets warmer in future, the precipitation trends will be more evident.

### ***Permafrost and Freeze-thaw Cycles***

Permafrost can be defined as a soil or rock that stays at or below a temperature of 0°C for a minimum period of two years [8], while an active soil layer is the one that freezes during winter and thaws during summer. Climate warming can lead to increase in soil temperature and this can result in the thickening of the active layers over the permanently frozen layers [9].

Canada's changing climate report [1] informs that the permafrost temperature has increased over the past 3 to 4 decades in Canada, and that regional observations have shown warming rates of about 0.1°C per decade in the central Mackenzie Valley and 0.3°C to 0.5°C per decade in the high Arctic. Such increments might seem modest, however, permafrost temperatures in these regions are already close to zero, therefore, the permafrost layer is highly vulnerable to thawing. Also, seasonal active layer thickness has increased by approximately 10% since 2000

in the Mackenzie Valley, making those areas more prone to deformations caused by freeze-thaw cycling.

The CCCR2019 report [1] also indicates some climate models that project large increments in the surface temperature across permafrost areas in Canada, which could result in a total increase of over 8°C in the mean surface temperature by the end of the 21<sup>st</sup> century. However, while air temperature predictions can be quite accurate, it is challenging to project associated reductions in permafrost extent from climate model simulations, because of unknown soil properties and ice content, and other uncertainties regarding the response of deep layers of permafrost (which can exceed hundreds of meters below surface).

There are several models simulating future reduction in permafrost extent, some being more pessimistic than others. For example, Kettles estimated that permafrost areas in Canada could be reduced by 43% under a 2°C to 5°C warming scenario [10], while Lawrence and Slater predicted that 90% of the near-surface permafrost in the Northern Hemisphere can disappear in the next 80 years [11]. However, a study developed by Zhang predicts a narrower range of permafrost reduction, from 20.5% to 24.4%, compared to air temperature increase from 2.8 to 7.0°C [12].

With the shortening of the freezing season due to climate change, locations where pavement layers have long frozen periods, such as the discontinuous permafrost areas, will likely suffer with more freezing and thawing cycles, and that might increase frost heave and differential thaw settlement. Another effect of the warming trend is that in southern areas of Canada, it is expected that pavement will suffer less with frost heave since frost penetration depth will decrease due to the shortening of the winter season [13].

## **Impact of Climate Change on Pavement Performance**

### ***Temperature***

Temperature as one of the most important components of the climate change factors plays a significant role on the performance of the flexible pavement. Higher pavement layer temperature can reduce the stiffness of asphalt materials and interrupt the proper spread of loads [14]. Moreover, increasing temperature due to climate change can accelerate the pavement ageing and development of cracks. Temperature can also indirectly affect the resilient modulus of granular layers and subgrade, since it will dictate when the water embedded in those materials is frozen or not, therefore, the seasonal resilient moduli of unbonded materials can vary according to both temperature and moisture conditions.

### ***Precipitation***

The moisture content of the flexible pavements is generally impacted by the precipitation and groundwater. Generally, moisture affects the flexible pavement by reducing the adhesion between binder and aggregates and initiating distresses such as stripping [15], [16]. Also, excessive moisture can cause a perceptible reduction in resilient modulus of unbound and subgrade materials [17]. Since ample moisture reduces the shear strength of the unbound and subgrade materials, it is expected to observe permanent deformation, rutting, and even failure of the flexible pavements under excessive precipitation [18], [19]. Studies also showed that flexible pavements with more fine aggregates are more likely to experience severe moisture

damages [17]. In AASHTO 93 design method, some of the variables that can account for the effect of higher soil moisture are the serviceability loss, soil resilient modulus, layer coefficients and drainage.

Some studies have correlated groundwater levels with precipitation and determined that the two variables tend to mirror each other with a delay [20], however, groundwater level trends are difficult to predict, due their complexity within the Canadian landscape and due to human withdrawals. One alternative could be to monitor the available data from provincial wells and look for local trends near the project site.

### ***Permafrost and Freeze-thaw Cycles Impacts***

The thawing of previously permanent frozen layers can cause serious damage to pavement structures. Settlement caused by thawing starts with a change in soil volume followed by a subsequent consolidation, in which the loads applied are transferred from the pore water to the soil skeleton. The degree of settlement will highly depend on the type of soil, density, pore water pressure generated and the soil's ability to compress. Subgrades rich in fine particles such as silt and clay, with access to capillary water, will usually present large settlements when loaded [21].

When a pavement reaches freezing conditions, the water trapped in the pavement will naturally freeze and expand. Therefore, heave can be identified as the upward displacement of the soil surface, led by transport processes under the surface as freezing occurs [22]. Certain types of soils can be more prone to heave, for example, silts and clays can produce very prominent heave, while sands and gravels not so much. Another factor that plays an important role is the groundwater table. Higher groundwater table levels can be correlated with greater frost heave damage.

Considering that one of the more severe climate change deterioration mechanisms can be attributed to freeze-thaw (FT) cycles, the increase in this event should be considered when designing and restoring pavements. One FT cycle can be considered as the fluctuation of the pavement's temperature, from above freezing to below freezing and then back to above freezing, and it can degrade the pavement structure through a few mechanisms, explained below.

First, when the weather reaches negative temperatures, the water trapped into the AC cracks and voids can freeze, expanding and damaging the aggregates and binder. This can cause stripping and raveling due to the loss of bond between aggregates in the asphalt concrete layer. Next, when temperature rises to positive, the water will melt and penetrate the unbonded layers. When the cycle starts over, the water that moved to the granular layers or subgrade will freeze again, possibly causing frost heave and depressions when melted.

Because the freeze-thaw cycle weakens the bond between aggregates in the asphalt concrete, it can also induce the asphalt mix to become softer, making it more susceptible to rutting and shoving [23]. Studies showed that the number of FT cycles can decrease the Marshall Stability by 77.4% after 24 days of cycles [24] and they can also cause a drastic decrease in tensile strength ratio when samples were subjected to a repeated number of cycles [25]. For a regular AC mix, rutting can be up to three times higher after 50 cycles of freezing and thawing, however, polymer modified mixes have presented a very positive performance under the FT cycles [26].

Even though there are a variety of studies relating FT cycles and damage mechanisms, there is no closed equation that relates the number of cycles and the decrease in the resilient modulus or any other stiffness measurement. Therefore, it is not yet possible to assertively predict the stiffness loss of asphalt concrete pavements under freezing and thawing cycles yet, since more research must be done in this field.

In AASHTO 93, the climatic region is not a direct structural design factor, but it can be very useful to provide information such as the frequency of the freeze-thaw cycle, the susceptibility of soil swelling, and moisture level from precipitation. With this information, frost heaving and soil swelling may be treated with a better drainage system or reflected in serviceability loss. The climatic region is also helpful in determining the proper pavement materials. For example, the asphalt concrete mix design can be improved by selecting the appropriate binder grade and aggregate source, but this part is not directly contained in the pavement structural design. Lastly, the serviceability loss should account for environmental impacts caused by frost heave and roadbed swelling, therefore, the increase in the number of FT cycles could also be incorporated in this variable.

Designers who follow the AASHTO 93 guide may not be aware that some material properties or pavement characteristics must be reselected or adjusted due to climate change. Without considering the impact of climate change on climate-related design inputs, the pavement may not meet performance expectations, resulting in more frequent maintenance and rehabilitation, early failure, and great economic losses.

## **Incorporation of Climate Change Predictions in Pavement Structural Design**

### ***Drainage Coefficients***

The drainage level is considered in AASHTO 93 by introducing the drainage coefficients ( $m_i$ ) in modifying the layer coefficient for the base and subbase courses and calculating the final Structural Number (SN) value. The  $m_i$  values are a function of the quality of drainage and percent of the time pavement structure is exposed to moisture levels. The percent of time pavement structure is exposed to moisture levels is affected by the average yearly rainfall and the prevailing drainage conditions. The recommended drainage coefficients for flexible pavement are provided in Table 1.

During the design process, it is up to the designers to determine the drainage level. When the impacts of future climate conditions are considered in the drainage design section, the drainage quality assumption must be made first, followed by selecting the exposure to moisture based on the average yearly rainfall and assumed prevailing drainage conditions [27].

Table 1: Recommended Drainage Coefficients ( $m_i$ ) for Flexible Pavements [5]

Quality of Drainage	Percent of Time Pavement Structure is Exposed to Moisture Levels Approaching Saturation			
	< 1%	1-5%	5-25%	> 25%
Excellent	1.40-1.35	1.35-1.30	1.30-1.20	1.20
Good	1.35-1.25	1.25-1.15	1.15-1.00	1.00
Fair	1.25-1.15	1.15-1.05	1.00-0.80	0.80
Poor	1.15-1.05	1.05-0.80	0.80-0.60	0.60
Very Poor	1.05-0.95	0.95-0.75	0.75-0.40	0.40

### Soil Resilient Modulus

One of the common methods to evaluate the stiffness of the unbound pavement materials is the resilient modulus ( $M_R$ ). The Federal Highway Administration (FHWA) defines this factor as “*the ratio of the applied cyclic stress to the recoverable (elastic) strain after many cycles of repeated loading*”. Besides direct laboratory tests, the  $M_R$  value can be derived from various methods and techniques, such as the R-value and CBR [5]. AASHTO 93 considers the seasonal effects on the resilient modulus through relative damage as presented in Equation 1.

$$u_f = 1.18 * 10^8 * M_R^{-2.32} \quad \text{Equation 1}$$

In which,  $u_f$  is the relative damage for a given modulus and  $M_R$  is the resilient modulus for a time period. Relative damages per month or per season can be yearly averaged and re-converted to  $M_R$  to produce the effective resilient modulus of a subgrade. This effective resilient modulus will then be used as an input for the pavement design.

Climate change can influence the soil resilient modulus through two main mechanisms: first, the warming temperatures due to climate change will shorten frozen periods. Secondly, the thawing phase can be more severe since the increase in precipitation levels could enhance soil saturation and decrease soil resistance. Therefore, when computing relative damage,  $u_f$ , the monthly or seasonally resilient modulus needs to be carefully estimated.

The groundwater table depth can vary significantly due to pumping of wells, evapotranspiration, and rainfall [28]. Monitoring wells are present all over Canada, for example, information on various collecting points can be found in the Provincial Groundwater Monitoring Network (PGMN) program, available at the Government of Ontario website. Mass volume parameters also play a decisive role in the modulus of a soil. The initial degree of saturation,  $S_{opt}$ , optimum volumetric water content,  $\theta_{opt}$ , and saturated volumetric water content,  $\theta_{sat}$  can be either obtained by direct laboratory tests, or through the gradation and engineering index properties.

The degree of soil moisture can also be called degree of saturation. During construction, the degree of saturation is usually under optimum conditions, however after some time, the degree of saturation tends to reach an equilibrium. This equilibrium degree of saturations is highly influenced by the groundwater table depth,  $y_{GWT}$ , and the soil-water characteristic curve, SWCC.

Depending on the temperature and moisture conditions, the soil can have degrees of saturation different than the equilibrium state, however, the soil will always tend to go back to equilibrium

with time, running cycles throughout the year seasons. The resilient modulus can be expressed as a function of soil saturation, according to Equation 2 [27]:

$$\log \frac{M_R}{M_{R_{opt}}} = a + \frac{b - a}{1 + \text{EXP} \left( \ln \frac{-b}{a} + k_m * (S - S_{opt}) \right)} \quad \text{Equation 2}$$

In which,  $\frac{M_R}{M_{R_{opt}}}$  is the Resilient modulus ratio;  $M_R$  is the resilient modulus at a given time and  $M_{R_{opt}}$  is the resilient modulus at a reference condition;  $a$  is the minimum of  $\log \frac{M_R}{M_{R_{opt}}}$ ;  $b$  is the maximum of  $\log \frac{M_R}{M_{R_{opt}}}$ ;  $k_m$  is the regression parameter;  $S - S_{opt}$  is the variation in degree of saturation expressed in decimal. The values of  $a$ ,  $b$ , and  $k_m$  varies for coarse-grained and fine-grained materials.

A good strategy, previously introduced by MEPDG, is to consider what stage the material is at, if it is frozen, thawing, or natural unfrozen. The frozen condition applies when the soil is under zero or negative temperatures, and the material will present high resilient modulus under this stage. Thawing conditions apply as soon as the temperature reaches positive values, and this period can be marked by the lowest modulus due to the high levels of saturation. After thawing started, the soil will gradually regain resistance. Finally, when the soil is completely recovered, it will enter an equilibrium stage, which can be called natural unfrozen.

Therefore, if the optimum resilient modulus  $M_{R_{opt}}$  is known, as well as the optimum degree of saturation, the moisture levels and temperature predictions under climate change conditions can be used to calculate the resilient modulus per month, or season. Then, the yearly average can be estimated through Equation 1. This simple strategy can be a good way to incorporate climate change predictions into the soil resilient modulus computation.

The same strategy can be used to estimate the yearly average resilient modulus of the base and sub-base layers. In this case, the fitting parameters  $a$ ,  $b$  and  $k_m$  must be adjusted for coarse-grained materials before being inputted into Equation 2.

### **Layer Coefficient**

Pavement layer coefficients are usually based on traditional materials coefficients, or more preferably derived from engineering values using correlation charts. AASHTO 93 recommends the asphalt concrete modulus to be measured at 20°C. This recommendation raises two main concerns: first, 20°C may not represent the average asphalt concrete temperature through the year in many locations. Second, it is not known how much damage extreme temperature variations can cause to a pavement when accumulated over a long period of time.

Since temperature can vary significantly during a year, hot summer days could result in pavements measuring more than 60°C. In such days, the asphalt concrete modulus will be significantly diminished, and the damage caused can be of noted importance when accumulated over time.

Two main strategies can be adopted when considering the influence of temperature warming due to climate change on asphalt modulus. The first strategy is to adjust the temperature according to climate change predictions for each region in Canada and pick the structural layer coefficient accordingly. The second strategy is to calculate the damage occurred over discrete short periods of time, considering the corresponding temperature and modulus at each stage, and adjust the pavement layer's thicknesses in case the damage limits are surpassed.

For unbonded granular layers, the structural coefficient is determined by charts. In this case, the resilient modulus can also be an input to find the structural coefficient. Therefore, the same procedure used to estimate the resilient modulus variation of soils due to temperature and moisture can be applied for the base and sub-base.

### ***Temperature Through Layers***

A model that accurately predicts the temperature of the pavement layers along the year is crucial for determining the materials modulus at each state. One of the very effective ways to estimate temperature profile on pavements is through the finite control volume method. The main inputs for this model are climatic data (air temperature and wind speed), meteorological data (solar radiation), and pavement surface radiation properties (albedo, emissivity, and absorption coefficients) [29].

One of the tools that can be used to estimate the temperature profile of pavements is the software TEMPS, that is, Temperature Estimate Model for Pavement Structures. This software uses the Finite Control Volume Method (FCVM) to forecast hourly temperatures at any depth in a pavement structure [30]. Climatic data such as the hourly solar radiation and monthly surface albedo can be downloaded from the National Solar Radiation Database (NSRDB) or Environment Canada.

### ***Case Study***

In this section an example will be presented to show how to incorporate climate change predictions into pavement design parameters.

#### **Case Study Site and Design Parameters:**

The study site is located at the provincial Highway 17 northwest of Pembroke, near the border of Ontario and Quebec. This section, indexed as 87-0901, was monitored by Long-term Pavement Performance (LTPP) Program of Federal Highway Administration (FHWA). The site was chosen considering that the section sits at the wet and freeze climatic zone and has well recorded pavement construction, structure, and performance information.

Basic project information is summarized in Table 2 retrieved from the LTPP database. Some design parameters were assumed based on common design practices, including the reliability level, combined standard error, and the drainage coefficient for asphalt surface layer. The design ESALs were calculated from traffic data computed by LTPP traffic module. Moreover, an effective subgrade resilient modulus  $M_R$  of 40.16 MPa was estimated based on other projects in the vicinity, and considering that the groundwater table depth was at 1m below the surface.

PAVEXpress is used in this study as it follows the AASHTO 93 design guide and provides a convenient user interface. The design parameters listed in Table 2 were used as inputs in the PAVEXpress calculation, resulting in the layer thickness of 152 mm, 228.6 mm and 660.4 mm

for asphalt surface, base, and subbase layer respectively. This structure is the base scenario of this study, and it is assumed to have been built in the year of 2020. Other four scenarios were considered in this research, and final comparisons and discussions were provided.

Table 2: Flexible Pavement Design Inputs (\*Retrieved from the LTPP database)

	Parameter	Value	Unit
Site Information	Latitude*	45.93325	
	Longitude*	-77.3358	
	Roadway classification*	Arterial; Rural	
Design Assumptions	Design period	20	Year
	Design ESALs	4478017	ESALs
	Reliability level (R)	85	%
	Combined standard error ( $S_0$ )	0.5	
	$P_i^*$	4.5	
	$P_t^*$	2.5	
Pavement Structure	AC $a_1$	0.375	
	AC $m_1$	1	
	Base thickness	228.6 (9)	mm (inch)
	Base $a_2$	0.2063	
	Base $m_2^*$	0.4	
	$E_B$	389.6 (56,507)	MPa (psi)
	Subbase thickness	660.4 (26)	mm (inch)
	Subbase $a_3$	0.1544	
	Subbase $m_3^*$	0.4	
	$E_{SB}$	163.9 (23,772)	MPa (psi)
	Subgrade effective $M_R$	40.16 (5,831)	MPa (psi)
	Subgrade optimum $M_R$	32.33 (468,907)	MPa (psi)
	Frozen Subgrade $M_R^*$	138 (20,015)	MPa (psi)

Scenario 1: Consideration of frost heave

In this scenario, it is assumed that the study site will be influenced by frost heave due to its climate region and climate change. Thus, to estimate the serviceability loss due to the frost heave,  $\Delta PSI_{FH}$ , the procedures described in the AASHTO 93 guide were followed. Some of the considerations were:

- The subgrade soil is a CL, 70% particles of which pass the N° 200 sieve, with a plasticity index (PI) of 12. Since the frost susceptibility classification for this soil is Very High, the frost heave rate ( $\phi$ ) was determined as 15.
- The drainage quality is “very poor” considering that the existing drainage coefficients for the base and subbase layers are 0.4, and a 5 feet of frost penetration depth was selected based on the site location. The two parameters result in a  $\Delta PSI_{SW-MAX}$  of 2.5.
- The frost heave probability (PF) was assumed as 50%.

With all parameters determined, the  $\Delta PSI_{FH}$  was calculated as 1.25. Therefore, the final  $\Delta PSI$  becomes  $P_i - P_t - \Delta PSI_{FH} = 4.5 - 2.5 - 1.25 = 1.25$ . The decrease in  $\Delta PSI$  from 2 to 1.25 resulted in an asphalt surface layer increase of 102 mm, when compared with the base scenario.

Scenario 2: Consideration of temperature and moisture damage caused by climate change

In this scenario, the affected design inputs are mainly the resilient modulus of the subgrade and modulus of elasticity of each pavement layer. The steps followed to adjust these material properties are summarized below.

1. Download 1 year temperature data from the chosen location.
2. Determine the hourly pavement temperature profile using TEMPS.
3. Determine  $\Delta t$  (number of hours since thawing started in each layer) and calculate the monthly average.
4. Determine a monthly environment adjustment factor ( $F_{env}$ ) for each granular layer, representing the frozen, recovering, and unfrozen conditions ( $F_f$ ,  $F_r$  and  $F_u$  respectively).
5. Calculate monthly values of elastic modulus for the base ( $E_B$ ), sub-base ( $E_{SB}$ ), and the monthly resilient modulus  $M_R$  for subgrade.
6. Input  $M_R$ ,  $E_B$  and  $E_{SB}$  monthly values into Equation 1 to calculate the pondered yearly modulus for each granular layer.
7. Use the yearly pondered modulus of base and sub-base to find  $a_2$  and  $a_3$ .

Steps used to adjust the asphalt concrete modulus are listed as follows.

1. With the same temperature data, and hourly profile extracted from TEMPS, determine the monthly temperature average of the AC layer.
2. Use hottest month average temperature to find the corresponding  $M_R$  of the asphalt layer and use this  $M_R$  to find  $a_1$ .

To obtain the pavement temperature profile, first the climatic data was downloaded from the National Solar Radiation Database (NSRDB). The data obtained at NSRDB was the air temperature, wind speed, solar radiation, and the surface albedo. The material properties of each pavement layer, such as the color, specific heat capacity, conductivity and density were defined according to Table 3.

Material Type	Identifier Color	Specific Heat Capacity (J/kg*K)	Conductivity (W/m*K)	Density (kg/m <sup>3</sup> )
AC	Black	1298	1.9	2374
Base	Gray	1038	3.73	2330
Sub-base	Gray	1131	4.065	2446
Subgrade	Gray	710	1.6	1550

Table 3: Material Property Definition at TEMPS

The next step was to define the climatic data, which includes hourly air temperature, wind speed and solar radiation, according to the downloaded materials from the National Solar Radiation Database (NSRDB). The hourly albedo values were also taken from the NSRDB Database and the monthly average was calculated to input in TEMPS.

This is followed by the definition of the pavement structure, that is, the thickness of the layers, and lastly by the generation of the pavement mesh. The mesh will determine how many points

the software will calculate for the temperature along the pavement depth. For this example, the mesh was chosen as 1 cm.

To estimate the resilient modulus of the materials under different circumstances, three main parameters are crucial, the percent passing No. 200 sieve,  $P_{200}$ , the effective grain size corresponding to 60% passing by weight,  $D_{60}$ , and the plasticity index (PI). Table 4 presents those three inputs considered for each unbonded layer. Note that these properties are the same as used in the base scenario.

**Table 4: Gradation and Properties of the Unbound Materials**

Layer	$P_{200}$ (%)	$D_{60}$ (%)	PI
Base	5	13.3	5
Sub-base	7.5	2	6
Subgrade	70	0.01	12

Referring to Equation 2, the parameters  $a$ ,  $b$ , and  $k_m$  varies for coarse-grained and fine-grained materials. Therefore, according to the MEPDG table 2.3.8, the base and sub-base  $a$ ,  $b$ , and  $k_m$  were defined as -0.3123, 0.3 and 6.8157, respectively, while the subgrade  $a$ ,  $b$ , and  $k_m$  was -0.5934, 0.4 and 0.1324. The drop in the resilient modulus due to the thawing of the pavement layers can be estimated through a reduction factor RF, as expressed in Equation 3 [27].

$$RF = \frac{M_{Rmin}}{\text{smaller of } (M_{Rfurnr}, M_{Ropt})} \quad \text{Equation 3}$$

Where,  $M_{Rfurnr}$  is the natural unfrozen resilient modulus and  $M_{Rmin}$  is the thawed resilient modulus, which corresponds to the weakest resilient modulus the material will present during the year. The subgrade frozen resilient modulus for this example was determined in the field and it is equal to 138 MPa [31].

The reduction of the soil stiffness with thawing is directly related to frost susceptibility, so the recommended reduction factor RF of the subgrade is dependent on the percent passing No. 200 sieve,  $P_{200}$ , and the plasticity index (PI). In the case study, the recommended factor is 0.55, according to the values suggested in the MEPDG manual. After thawing, the soil will gradually start to gain resistance. This process can be represented by the recovery ratio RR, which can be described by the number of hours elapsed since thawing started ( $\Delta t$ ) divided by the number of hours required for the material to recover ( $T_R$ ), according to Equation 4 [27].

$$RR = \frac{\Delta t}{T_R} \quad \text{Equation 4}$$

The number of hours required for the material to recover ( $T_R$ ) varies according to the material properties. For the case study, the subgrade was considered to have a  $T_R$  equal to 120 days, that is the recommended value for any material with  $0.1 < P_{200} * PI < 10$  [27].

To estimate the resilient modulus at each pavement stage, that is, frozen, thawing, or natural unfrozen, an environmental adjustment factor  $F_{env}$  can be used. This factor can estimate the resilient modulus  $M_R$  at any time or position, when multiplied by the resilient modulus at optimum conditions, as expressed in Equation 5.

$$M_R = F_{env} * M_{Ropt} \quad \text{Equation 5}$$

Where,  $F_{env}$  is the adjustment factor, and  $M_{Ropt}$  is the resilient modulus at optimum conditions. The number of hours elapsed since thawing started ( $\Delta t$ ) is the key to define  $F_{env}$ . If  $\Delta t$  is equal to 0, the soil is frozen, therefore  $F_{env}$  is equal to  $F_f$ , if  $\Delta t$  is between 0 and 2880 hours (120 days), then  $F_{env}$  is equal to  $F_r$ , which means that the soil is under the recovery period, and if  $\Delta t$  is greater than 2880 hours, it means that the soil has already recovered and is unfrozen, therefore,  $F_{env}$  is equal to  $F_u$ . The steps to compute  $F_f$ ,  $F_r$  and  $F_u$  are described in the MEPDG manual.

Scenario 2 is further broken into 3 sub-scenarios, as described below:

- Scenario 2.1 assumes the temperatures remain unchanged throughout the 20-years performance period and the ground water table is at 0.5 m below subgrade surface.
- Scenario 2.2 considers a temperature increase of 15.08% and the ground water table at 1 m below subgrade surface.
- Scenario 2.3 considers a temperature increase of 15.08% and the ground water table at 0.5 m below subgrade surface.

The temperature increase of 15.08% is chosen from temperature projection at the study site, in which the data was downloaded from ClimateData.ca, for a performance period of 20 years starting in 2020, under RCP 4.5. Following the steps mentioned previously, the subgrade resilient modulus was calculated for the three scenarios, as shown in Table 5. Note that the last row is the Effective  $M_R$ , which is determined through Equation 1.

Table 5: Subgrade  $M_R$  Variations for Each Scenario (unit: MPa)

Month	Base	Scenario 2.1	Scenario 2.2	Scenario 2.3
Jan	138	138	138	138
Feb	138	138	138	138
Mar	138	138	138	138
Apr	95	92	93	90
May	23	13	22	12
Jun	27	12	27	12
Jul	32	14	32	14
Aug	38	16	38	16
Sep	45	18	45	18
Oct	45	18	45	18
Nov	45	18	45	18
Dec	66	53	73	61
Effective $M_R$	40.16	18.76	39.75	18.44

The subgrade  $M_R$  was found to be constant through the months of January, February, and March, due to the frozen period, which according to field data had a resilient modulus of 138 MPa. On the other hand, from April to December the results showed interesting variations according to each scenario. When the water table depth was kept constant and the temperature increased by 15.08%, it is possible to notice that the temperature alone had low impact on the

resilient modulus of the subgrade. That became evident, since when comparing the base scenario and 2.2, there is an effective resilient modulus decrease of only 1.02%, while in scenarios 2.1 and 2.3 the decrease was 1.7%. The impact of moisture variation, however, is much higher. In the simulations, if the water table depth goes from 1 m to 0.5 m below the subgrade surface, the effective resilient modulus of the subgrade can become 53.3% lower, comparing the base scenario and 2.1, and 53.6% lower, comparing scenarios 2.2 and 2.3.

The variations in the base and subbase layer modulus of elasticity along the year for the four studied scenarios can be seen in Table 6 and

Table 7. The crushed granular base layer presented no change in the resilient modulus when varying the ground water table depth and the variation in the modulus due to temperature increase was less than 1%. This was expected since this is a coarse layer, and the ground water table depth is far from the base in all scenarios. The findings for the sub-base layer are very similar to the base. The uncrushed granular sub-base layer presented no change in the resilient modulus when varying the ground water table depth and the variation in the modulus due to temperature increase was less than 1%. In summary, the design moduli for the granular pavement layers are listed in Table 8.

Table 6: Base Layer Modulus of Elasticity Variations for Each Scenario (unit: MPa)

Month	Base	Scenario 2.1	Scenario 2.2	Scenario 2.3
Jan	6894.8	6894.8	6894.8	6894.8
Feb	6894.8	6894.8	6894.8	6894.8
Mar	6894.8	6894.8	6894.8	6894.8
Apr	1557.2	1557.2	1556.4	1556.4
May	250.0	250.0	248.6	248.6
Jun	282.3	282.3	280.8	280.8
Jul	314.6	314.6	313.1	313.1
Aug	341.2	341.2	340.6	340.6
Sep	342.8	342.8	342.8	342.8
Oct	342.8	342.8	342.8	342.8
Nov	342.8	342.8	342.8	342.8
Dec	3245.2	3245.2	4113.1	4113.1
<b>M<sub>BS</sub></b>	<b>389.6</b>	<b>389.6</b>	<b>388.4</b>	<b>388.4</b>

Table 7: Subbase Layer Modulus of Elasticity Variations for Each Scenario (unit: MPa)

Month	Base	Scenario 2.1	Scenario 2.2	Scenario 2.3
Jan	6894.8	6894.8	6894.8	6894.8
Feb	6894.8	6894.8	6894.8	6894.8
Mar	6894.8	6894.8	6894.8	6894.8
Apr	1441.2	1441.2	1441.1	1441.1
May	94.1	94.1	93.9	93.9
Jun	114.7	114.7	114.5	114.5
Jul	135.3	135.3	135.1	135.1
Aug	153.9	153.9	153.8	153.8
Sep	156.1	156.1	156.1	156.1
Oct	156.1	156.1	156.1	156.1
Nov	156.1	156.1	156.1	156.1
Dec	2826.7	2826.7	2823.8	2823.8
<b>M<sub>SB</sub></b>	<b>163.9</b>	<b>163.9</b>	<b>163.7</b>	<b>163.7</b>

Table 8: Resilient Modulus in MPa (psi) for Base, Subbase and Subgrade in Each Scenario

Scenario	Description	Base	Sub-base	Subgrade
Base	Temperature of 2020, ground water table at 1m below subgrade surface	389.6 (56,507)	163.9 (23,772)	40.2 (5,831)
1	Same as Base Scenario, under frost heave effect	389.6 (56,507)	163.9 (23,772)	40.2 (5,831)
2.1	Temperature of 2020, ground water table at 0.5 m below subgrade surface	389.6 (56,507)	163.9 (23,772)	18.8 (2,727)
2.2	Temperature increases 15.08%, ground water table at 1m below subgrade surface	388.4 (56,333)	163.7 (23,743)	39.7 (5,758)
2.3	Temperature increases 15.08%, ground water table at 0.5m below subgrade surface	388.4 (56,333)	163.7 (23,743)	18.4 (2,669)

It can be concluded from this analysis that the resilient modulus of the base and sub-base layers is not very sensitive to the temperature increase and fluctuations in ground water level. This is expected, since base and sub-base layers are coarse materials, and their constitution is made to be less susceptible to the effects of moisture and frost penetration. The subgrade, on the other hand, is very sensitive to fluctuations in the ground water table depth, since this alters the soil moisture, and consequently the stiffness. The temperature rise will have a small impact on the soil's performance, as expected, since the temperature rise will only shift the muddy season to earlier periods in the year, and after the recovery period, the soil will maintain the equilibrium modulus. This scenario could be totally different in northern territories since the temperature rise can result in the melting of permafrost layers in the warm seasons.

Because the moduli have changed under the four scenarios, the layer coefficient should also be updated. The updated layer coefficients for the base ( $a_2$ ) and subbase layers ( $a_3$ ) are computed as shown in Table 9.

Table 9: Layer Coefficients for the Base and Subbase Layers under All Scenarios

Scenario	a <sub>2</sub>	a <sub>3</sub>
Base	0.2063	0.1544
2.1	0.2063	0.1544
2.2	0.2059	0.1542
2.3	0.2059	0.1542

Moreover, to calculate the asphalt concrete (AC) modulus of elasticity at different temperature, data related to the materials properties, such as the initial air voids and gradation had to be used. The data used for this example comes from a real asphalt concrete analyzed at the Centre for Pavement and Transportation Technology and is consistent with a high strength asphalt concrete sample. The material's properties are:

- Initial air voids = 3.9%
- Viscosity parameters: A = 9.715, VTS = -3.217
- Original binder viscosity at 77°C = 0.93 cP
- Depth = 0.25 in, or 0.635 cm
- Effective asphalt content, Percent by total mixture volume = 12.6%
- Cumulative percent retained on ¾ sieve, P<sub>¾</sub> = 0%
- Cumulative percent retained on 3/8 sieve, P<sub>3/8</sub> = 19.70%
- Cumulative percent retained on #4 sieve, P<sub>4</sub> = 45.70%
- Percent passing #200 sieve, P<sub>200</sub> = 3%

Because the resilient modulus of the AC is dependent on the loading frequency, a vehicle speed, weight, and tire pressure had to be assumed. A truck axle weight of 5,443 kilograms was considered in this analysis, the tire pressure was assumed to be 0.76 Mpa and the vehicle speed as 70km/h.

The hourly asphalt concrete temperature calculated through TEMPS was used to compute the temperature in the AC layer. The master curve used to relate temperature and the resilient modulus of the asphalt concrete was developed using Equation 6, from the information available from material specifications and volumetric design of the mixture [27].

$$\begin{aligned}
 & \log(E^*) \\
 & = 3.750063 + 0.02932\rho_{200} - 0.001767(\rho_{200})^2 - 0.002841\rho_4 - 0.058097V_a \\
 & - 0.802208 \left( \frac{V_{beff}}{V_{beff} + V_a} \right) \\
 & + \frac{3.871977 - 0.0021\rho_4 + 0.003958\rho_{38} - 0.000017(\rho_{38})^2 + 0.005470\rho_{34}}{1 + e^{(-0.603313 - 0.313351 \log(f) - 0.393532 \log(\eta))}}
 \end{aligned}
 \tag{Equation 6}$$

In which,

- $\eta$  = bitumen viscosity, 10<sup>6</sup> Poise;
- $f$  = loading frequency, Hz;
- $V_a$  = air void content, %;

- $V_{beff}$  = effective bitumen content, % by volume;
- $\rho_{34}$  = cumulative % retained on the  $\frac{3}{4}$  in sieve;
- $\rho_{38}$  = cumulative % retained on the  $\frac{3}{8}$  in sieve;
- $\rho_4$  = cumulative % retained on the No. 4 sieve;
- $\rho_{200}$  = % passing the No. 200 sieve.

The bitumen viscosity under the studied temperature was calculated and imputed in the dynamic modulus master curve. The equations used in this example to find the bitumen viscosity can be found at the MEPDG Manual.

The average modulus of the hottest month of the year (July) was used to calculate the layer coefficient for pavement structural design. The average modulus in the base scenario was calculated as 2,136 MPa, while the average modulus for the 15.08% temperature increase was 1,843 MPa, a decrease of 14% in the AC stiffness.

Once the AC elastic modulus was determined, the layer coefficient for pavement structural design was estimated using Figure 2.5 of the AASHTO 93 guide as approximately 0.375 and 0.34 corresponding to the  $E_{AC}$  of 2,136 and 1,843 MPa. Finally, the adjusted design moduli were used to calculate the layer thickness for the Scenario 2.1 to 2.3. A summary of pavement structure is provided in Table 10, including all studied scenarios. Note that the thicknesses of the base and subbase layers were kept constant for all scenarios, so the difference in design is reflected by the thickness of the AC layer.

Table 10: Layer Thickness Comparisons under Different Design Scenarios in mm (inch)

Parameter	Scenario				
	Base	1	2.1	2.2	2.3
AC	152 (6)	254 (10)	229 (9)	165 (6.5)	254 (10)
Base	229 (9)	229 (9)	229 (9)	229 (9)	229 (9)
Subbase	660 (26)	660 (26)	660 (26)	660 (26)	660 (26)
Required Minimum SN	4.5	6.05	5.7	4.5	5.7
Total SN	4.6	6.1	5.72	4.55	5.74

From the table above, major findings can be summarized as below.

- The consideration of frost heave can increase the required minimum SN, leading to thicker AC layer. This can be seen by comparing the Base Scenario with Scenario 1.
- If temperature rise by the climate change is considered, the AC thickness has to be increased. This conclusion is reached by comparing the base scenario with 2.2 and comparing Scenario 2.1 with 2.3.
- The climate change may cause the ground water table to rise, so Scenario 2.1 and 2.3 are included in the analysis assuming the ground water table has risen from 1 m to 0.5 m below the subgrade surface. By comparing the base scenario with 2.1 or Scenario 2.2 with 2.3, one can see a significant thickness increase in the AC layer. As mentioned in the previous section, this is caused by the noticeable decrease of subgrade resilient modulus.

## Conclusion

This research assessed the impacts of climate change in flexible pavements in Canada by addressing climate projections and its consequences around the country. The study also proposed a methodology for the incorporation of climatic projected changes in the design of flexible pavements through AASHTO 93. An example was performed to illustrate the incorporation of the climate change parameters, including temperature, precipitation/moisture, and freeze-thaw cycles. The serviceability index, drainage coefficients, soil (subgrade) resilient modulus, and layer coefficients were found to be the most sensitive pavement design parameters. In the case study, the temperature increase was 15% in a design period of 20 years, but the proposed method for considering temperature rise can be applied for different locations and any climate change projections. The results showed that temperature alone had a low impact on the structural design, however, the climate change impacts were high when associated with an increase in moisture levels. The impacts of temperature alone, however, can be much higher in the areas affected by permafrost thawing.

## References

- [1] Environment and Climate Change Canada, "Canada's Changing Climate Report," 2019.
- [2] B. Mills, J. Andrey, J. Smith, S. Parm and K. Huen, "Road Well-Traveled: Implications of Climate Change for Pavement Infrastructure in Southern Canada," *Transportation Association of Canada (TAC)*, 2007.
- [3] S. L. Tighe, J. Smith, , B. Mills and J. Andrey, "Using the MEPDG to Assess Climate Change Impacts on Southern Canadian Roads," in *Seventh International Conference on Managing Pavement Assets*, 2008.
- [4] J. T. Smith, S. L. Tighe, J. C. Andrey and B. Mil, "Temperature and Precipitation Sensitivity Analysis on Pavement Performance - Report No. Weather 08-019," in *Fourth National Conference on Surface Transportation Weather; Seventh International Symposium on Snow Removal and Ice Control Technology*, 2008.
- [5] American Association of State Highway and Transportation Officials, "AASHTO Guide for Design of pavement structures," in *Proceedings of the International Conference on Sustainable Waste Management and Recycling: Construction Demolition Waste*, 1993.
- [6] Environment Canada, "A state of the environment report: The state of Canada's climate: monitoring variability and change (SOE Report No. 95-1. ISBN 0-662-23061-2. Cat. No. En1-11/95-1E)," Government of Canada, 1995.
- [7] S. Westra, L. V. Alexander and F. W. Zwiers, "Global increasing trends in annual maximum daily precipitation," *Journal of climate*, vol. 26, no. 11, pp. 3904-3918, 2013.
- [8] P. J. Williams, "Permafrost and climate change: geotechnical implications," *Philosophical Transactions of the Royal Society of London. Series A: Physical and Engineering Sciences*, vol. 352, no. 1699, pp. 347-358, 1995.

- [9] H. Batenipour, "Understanding the performance of highway embankments on degraded permafrost," University of Manitoba (Canada), 2012.
- [10] I. M. Kettles, C. Tarnocai and S. D. Bauke, "Predicted permafrost distribution in Canada under a climate warming scenario," *Current Research, Geological Survey of Canada, 1997-E*, pp. 109-115, 1997.
- [11] D. M. Lawrence and A. G. Slater, "A projection of severe near-surface permafrost degradation during the 21st century," *Geophysical Research Letters*, vol. 32, no. 24, 2005.
- [12] Y. Zhang, W. Chen and D. W. Riseborough., "Disequilibrium response of permafrost thaw to climate warming in Canada over 1850–2100," *Geophysical Research Letters*, vol. 35(2), 2008.
- [13] J. S. Daniel and e. al, "Climate change: potential impacts on frost–thaw conditions and seasonal load restriction timing for low-volume roadways," *Road Materials and Pavement Design*, vol. 19, no. 5, pp. 1126-1146, 2018.
- [14] American Association of State Highway and Transportation Officials, "Mechanistic-empirical pavement design guide: a manual of practice," 2008.
- [15] A. K. Apeagyei, J. R. Grenfell and G. D. Airey, "Influence of aggregate absorption and diffusion properties on moisture damage in asphalt mixtures," *Road Materials and Pavement Design*, vol. 16, no. sup1, pp. 404-422, 2015.
- [16] P. S. Kandahl and I. J. Richards., "Premature failure of asphalt overlays from stripping: Case histories," National Center for Asphalt Technology (US), 2001.
- [17] A. Dawson, "Water in Road Structures," Dordrecht: Springer Netherlands, 2009.
- [18] L. Korkiala-Tanttu, "Speed and reloading effects on pavement rutting," in *Proceedings of the Institution of Civil Engineers-Geotechnical Engineering*, 2007.
- [19] H. L. Theyse, "A mechanistic-empirical design model for unbound granular pavement layers," University of Johannesburg, 2008.
- [20] Z. Chen, S. E. Grasby and K. G. Osa, "Predicting average annual groundwater levels from climatic variables: an empirical model," *Journal of Hydrology*, vol. 260, pp. 102-117, 2002.
- [21] E. Simonsen and U. Isacsson, "Thaw weakening of pavement structures in cold regions," *Cold regions science and technology*, vol. 29, no. 2, pp. 135-151, 1999.
- [22] K. O'Neill and R. D. Miller, "Exploration of a rigid ice model of frost heave," *Water Resources Research*, vol. 21, no. 3, pp. 281-296, 1985.
- [23] E. A. Abreu, "Impacts of Climate Change on Canadian Airport Pavements," University of Waterloo, 2019.
- [24] E. Özgan and S. Serin, "Investigation of certain engineering characteristics of asphalt

- concrete exposed to freeze–thaw cycles," *Cold Regions Science and Technology*, vol. 85, pp. 131-136, 2013.
- [25] D. Feng and e. al., "Impact of salt and freeze–thaw cycles on performance of asphalt mixtures in coastal frozen region of China," *Cold Regions Science and Technology*, vol. 62, no. 1, pp. 34-41, 2010.
- [26] W. Si and e. al., "Impact of freeze-thaw cycles on compressive characteristics of asphalt mixture in cold regions," *Journal of Wuhan University of Technology-Mater*, vol. 30, no. 4, pp. 703-709, 2015.
- [27] Applied Research Associates Inc. ERES Division, "Guide for Mechanistic-Empirical Design of New and Rehabilitated Pavement Structures Appendix DD-1: Resilient Modulus as Function of Soil Moisture-Summary of Predictive Models - Final Document," Champaign, IL, 2000.
- [28] H. Simpson, "Ground Water - An Important Rural Resource, Understanding Groundwater," Queen's Printer for Ontario - Ministry of Agriculture, Food and Rural Affairs, 2015.
- [29] M. Z. Alavi, M. R. Pouranian and E. Y. Hajj, "Prediction of asphalt pavement temperature profile with finite control volume method," *Transportation Research Record*, vol. 2456, no. 1, pp. 96-106, 2014.
- [30] W. Liu and e. al, "Stormwater runoff and pollution retention performances of permeable pavements and the effects of structural factors," *Environmental Science and Pollution Research*, vol. 27, pp. 30831-30843, 2020.
- [31] L. D'Amours and e. al., "Assessment of Subgrade Soils for Pavement Design for Highway 407, East Extension Pickering to Oshawa, Ontario," in *TAC 2016: Efficient Transportation-Managing the Demand-2016 Conference and Exhibition of the Transportation Association of Canada*, 2016.